



Cite this: *Chem. Commun.*, 2020, **56**, 12138

Received 20th July 2020,  
Accepted 7th September 2020

DOI: 10.1039/d0cc04967k

[rsc.li/chemcomm](http://rsc.li/chemcomm)

**The synthesis of strongly solubilising multibranched aliphatic side chains for  $\pi$ -conjugated polymers is reported. The solubilising capability of the side chains and their effect on the polymer properties are studied on the example of copolymers composed of up to six unsubstituted, 'unshielded' thiophene units per side chain-substituted naphthalene diimide unit.**

$\pi$ -Conjugated polymers have been widely studied as organic semiconductors for applications such as solar cells, thin-film transistors and light-emitting diodes.<sup>1,2</sup> A key advantage of  $\pi$ -conjugated polymers and other organic semiconductors over their inorganic counterparts is their processability from solution. For conjugated polymers, this property is usually achieved by attaching aliphatic side chains to the  $\pi$ -conjugated backbone, modifying the interchain packing and enabling solubility in organic solvents.<sup>3–5</sup> The attachment of linear side chains such as hexyl or octyl chains can often sufficiently solubilize the polymers, but for polymers with more rigid, planar conjugated backbones or donor–acceptor copolymers with strong intermolecular interactions, branched instead of linear aliphatic side chains are usually required to achieve good solubility.<sup>6</sup> 2-Ethylhexyl or 2-octyldodecyl (2OD) chains are among the most popular branched aliphatic side chains.<sup>3</sup>

While many well-investigated  $\pi$ -conjugated polymers such as poly(3-hexylthiophene) (P3HT) or poly(9,9-dioctylfluorene-*alt*-benzothiadiazole) (F8BT) feature aliphatic side chains on every or every other unit of the conjugated backbone, some

<sup>a</sup> Department of Chemistry and Centre for Processable Electronics, Imperial College London, Molecular Sciences Research Hub, 80 Wood Lane, London W12 0BZ, UK.  
E-mail: [f.glockhofer@imperial.ac.uk](mailto:f.glockhofer@imperial.ac.uk), [m.heeney@imperial.ac.uk](mailto:m.heeney@imperial.ac.uk)

<sup>b</sup> School of Materials Science and Engineering, Tianjin University, Tianjin 300072, P. R. China

<sup>c</sup> Institute of Molecular Plus, Tianjin Key Laboratory of Molecular Optoelectronic Science, Tianjin University, Tianjin 300072, P. R. China

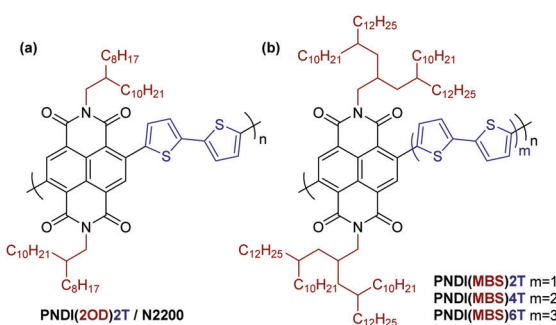
† Electronic supplementary information (ESI) available: Synthetic details, thermal analysis, solubility tests, UV-vis absorption, photoluminescence, cyclic voltammetry, <sup>1</sup>H and <sup>13</sup>C NMR spectra. See DOI: [10.1039/d0cc04967k](https://doi.org/10.1039/d0cc04967k)

## Multibranched aliphatic side chains for $\pi$ -conjugated polymers with a high density of 'unshielded' aromatics†

Simeng Wang,<sup>a</sup> Jessica Shaw,<sup>a</sup> Yang Han,<sup>b</sup> Zhuping Fei,<sup>c</sup> Florian Glöcklhofer<sup>ID \*a</sup> and Martin Heeney<sup>ID \*a</sup>

polymers are composed of two or even three unsubstituted aromatic units per side chain-substituted unit. Poly(9-(1-octynonyl)carbazole-*alt*-4,7-dithienylbenzothiadiazole) (PCDTBT) and copolymers of naphthalene diimide (NDI) and bithiophene (2T), such as **PNDI(2OD)2T** (Scheme 1a), are two examples of such polymers that show good performance in organic solar cells or transistors.<sup>7,8</sup>

Interestingly, although attaching simple branched aliphatic side chains is well investigated, the attachment of side chains with multiple branching point has, to the best of our knowledge, not yet been reported. Such multibranched aliphatic side chains (MBS) potentially offer further increased solubilizing capability, allowing for the synthesis of soluble polymers with a higher density of unsubstituted aromatic units in the conjugated backbone than with previously reported side chains. A high density of unsubstituted, 'unshielded' aromatics in the backbone may have a beneficial effect on various applications: it may allow for closer interaction with other semiconductors, dopant molecules, and analytes (if used in sensors) and may even improve the photocatalytic performance of the polymers.<sup>9</sup>



**Scheme 1** (a) Structure of **PNDI(2OD)2T**. (b) Structures of target compounds with 4-decyl-2-(2-decyltetradecyl)hexadecyl chains as multibranched aliphatic side chains (MBS) and up to six unsubstituted thiophene units.



Here we report a simple synthetic route to an MBS with three branching points, 4-decyl-2-(2-decyltetradecyl)hexadecyl, and study its solubilizing capability and effect on the properties of a series of  $\pi$ -conjugated polymers as an important first step towards an investigation in above-mentioned applications. We aimed to introduce the side chain in donor–acceptor copolymers composed of NDI and unsubstituted thiophene units and to gradually increase the number of thiophene units per NDI from two, as in **PNDI(2OD)2T**, to four and six (Scheme 1b). As mentioned, such donor–acceptor copolymers are often difficult to dissolve as a result of strong intermolecular interactions and NDI-thiophene copolymers are no exception in this regard.<sup>10</sup> Furthermore, the solubility of unsubstituted oligothiophenes decreases rapidly when increasing the number of repeat units.

For introducing the MBS in the NDI unit, we synthesized the respective amine **MBS-NH<sub>2</sub>** **3** in just two steps (Scheme 2a). In the first step, acetonitrile ( $\text{CH}_3\text{CN}$ ) was dialkylated with 1-bromo-2-decyltetradecane **1** to give the multibranched aliphatic nitrile **2** in 30% yield following column chromatography. This reaction was inspired by previous reports of (mono)alkylation of acetonitrile<sup>11–13</sup> and, in our case, is considered to proceed in two consecutive deprotonation and alkylation steps. *n*-Butyllithium (*n*-BuLi) served as the base for the initial deprotonation of  $\text{CH}_3\text{CN}$  in our reaction. An excess (2.5 eq.) of the deprotonated  $\text{CH}_3\text{CN}$  was then reacted with alkyl bromide **1**, with the deprotonated  $\text{CH}_3\text{CN}$  also serving as a base for a subsequent second deprotonation and alkylation. Nitrile **2** was then reduced to the amine **3** in the second step of the synthesis. Using LiAlH<sub>4</sub> for the reduction, crude amine **3** was obtained in a yield of 90% and used for the synthesis of monomer **M1** without further purification.

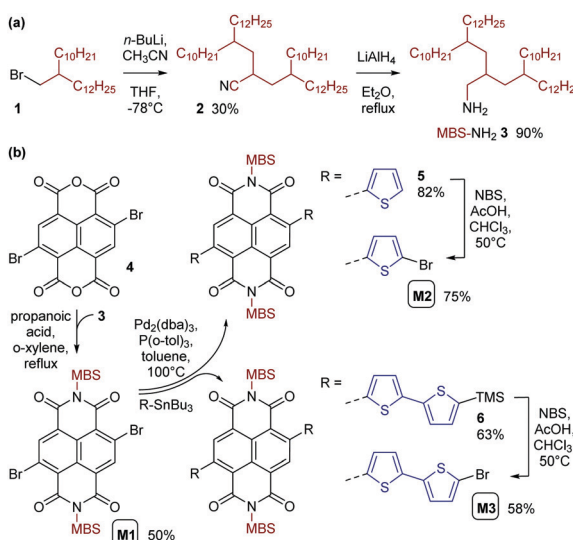
Monomer **M1** was obtained by reacting 2,6-dibromonaphthalene-1,4,5,8-tetracarboxylic dianhydride **4** with amine **3** under conditions previously used for the introduction of monobranched aliphatic

side chains (Scheme 2b).<sup>14</sup> Purification by column chromatography afforded pure monomer **M1** as an orange viscous oil in 50% yield. **M1** was then used for Stille polymerization with distannylated bithiophene **TT**, giving the dark blue polymer **PNDI(MBS)2T** in good yields (Scheme 3a). However, **M1** was also used for the synthesis of monomers **M2** and **M3** by Stille coupling with monostannylated (bi)thiophenes, yielding compounds **5** and **6**, and subsequent bromination (Scheme 2b). Stille polymerization of these monomers with **TT** afforded the dark green polymers **PNDI(MBS)4T** and **PNDI(MBS)6T** (Scheme 3a). In this synthetic approach, which was previously used for the synthesis of **PNDI(2OD)4T**,<sup>15,16</sup> the additional thiophene units of the polymers are introduced in the NDI comonomer, as opposed to extending the distannylated bithiophene comonomer **TT**. Direct arylation polycondensation of **M1** and the respective oligothiophenes may be a suitable alternative approach, considering previous reports.<sup>17</sup>

All polymerizations were performed in a microwave oven in a reaction time of approx. 50 min, gradually increasing the temperature from 100 °C to 200 °C. As for the Stille reactions towards compounds **5** and **6**,  $\text{Pd}_2(\text{dba})_3$  and tri(*o*-tolyl)phosphine was used as the catalytic system for the polymerizations. The yields given in Scheme 3a represent the soluble polymer fractions obtained by Soxhlet extraction with hexane (for **PNDI(MBS)2T**, **PNDI(MBS)4T**) or chloroform (for **PNDI(MBS)6T**). Medium to high molecular weight polymers were obtained (gel permeation chromatography (GPC) data provided in Scheme 3a). The higher molecular weight and dispersity ( $D$ ) observed for **PNDI(MBS)6T** can be attributed to the use of the better solvent chloroform instead hexane for the final Soxhlet extraction step of this polymer.

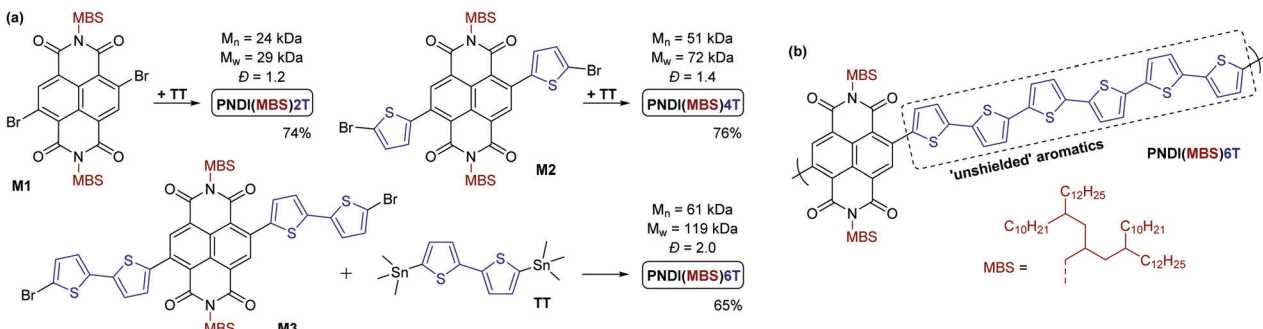
Thermogravimetric analysis (TGA) revealed the high thermal stability of the polymers, with the decomposition starting above 400 °C in all three cases and a 5% mass loss between 447 °C and 450 °C (Fig. S7, ESI†). For **PNDI(MBS)4T** and **PNDI(MBS)6T**, differential scanning calorimetry (DSC) (Fig. S8, ESI†) showed endothermic transitions on heating with peaks at 177 °C and 176 °C, respectively, and exothermic transitions with peaks at 157 °C and 160 °C on cooling. These transitions can be attributed to melting and crystallization of the polymers. Broad, lower temperature transitions are also observed for these polymers (midpoints at 91 °C/61 °C on heating/cooling) possibly corresponding to glass transitions. No transitions were observed for **PNDI(MBS)2T**. Comparison to **PNDI(2OD)2T**, for which a 5% mass loss at approx. 450 °C,<sup>18</sup> a glass transition at 74 °C,<sup>19</sup> and a molecular weight dependent melting point between 280 and 310 °C were reported,<sup>17</sup> confirmed that the MBS does not affect the stability of the polymers but has a pronounced effect on the other thermal transitions.

To evaluate the solubilizing capability of the MBS, we tested the solubility of the polymers in chlorobenzene (CB), a solvent often used for processing conjugated polymers from solution, and in *n*-hexane. For **PNDI(MBS)2T**, we found the solubility to be  $>200 \text{ g L}^{-1}$  in CB and  $>20 \text{ g L}^{-1}$  in *n*-hexane, a surprising observation considering that the latter is known to be a very poor solvent for conjugated polymers. For **PNDI(MBS)4T**, the



**Scheme 2** (a) Synthesis of multibranched aliphatic amine **3**. (b) Synthesis of monomers **M1–3** using amine **3** for the introduction of the multibranched aliphatic side chains (MBS).





**Scheme 3** (a) Stille copolymerization of monomers **M1**, **M2**, and **M3** with distannylated bithiophene **TT** yielding polymers **PNDI(MBS)2T**, **PNDI(MBS)4T**, and **PNDI(MBS)6T**, respectively. Polymerization conditions:  $\text{Pd}_2(\text{dba})_3$ ,  $\text{P}(\text{o-tol})_3$ , chlorobenzene,  $100\text{ }^\circ\text{C} \rightarrow 200\text{ }^\circ\text{C}$ , microwave oven. (b) Structure of **PNDI(MBS)6T** with highlighted unsubstituted, 'unshielded' thiophene units.

solubility was found to be approx.  $100\text{ g L}^{-1}$  in CB and  $8\text{ g L}^{-1}$  in *n*-hexane. **PNDI(MBS)6T** could not be dissolved in *n*-hexane, but the solubility in CB was approx.  $70\text{ g L}^{-1}$ , despite the high density of unsubstituted thiophene units. For **PNDI(2OD)2T**, our tests showed a lower solubility of  $25\text{ g L}^{-1}$  in CB. Previously, "solubilities [...] in conventional organic solvents such as xylene and dichlorobenzene (DCB) as high as  $60\text{ g L}^{-1}$ " were reported, possibly reflecting molecular weight differences.<sup>8</sup>

UV-vis absorption spectra (Fig. 1) in CB showed an absorption maximum at  $368\text{ nm}$  and a charge-transfer (CT) absorption band with a peak at  $617\text{ nm}$  for **PNDI(MBS)2T**. The peaks are clearly blueshifted compared to **PNDI(2OD)2T**, which (despite having the same  $\pi$ -conjugated backbone) showed peaks at  $394$  and  $706\text{ nm}$  in the same solvent (Fig. S9, ESI<sup>†</sup>). This blueshift indicates considerably reduced aggregation of **PNDI(MBS)2T** in CB as a result of the MBS, a conclusion further supported by the fact that the absorption peaks of **PNDI(2OD)2T** shifted to similar values (approx.  $370$  and  $620\text{ nm}$ ) when measured in chloronaphthalene (CN), a solvent known to suppress aggregation.<sup>20</sup> For **PNDI(MBS)2T** no further blueshift was observed when measured in CN and at lower concentrations in CB (Fig. S11, ESI<sup>†</sup>).

Measuring **PNDI(MBS)4T** and **PNDI(MBS)6T** in CB, we observed a redshift of both peaks with an increasing density of thiophene units. Compared to **PNDI(MBS)2T**, the peaks in the spectrum of **PNDI(MBS)4T** redshifted by  $26$  and  $19\text{ nm}$ , followed by a redshift of another  $63$  and  $31\text{ nm}$  in **PNDI(MBS)6T**. Similarly, the absorption onset shifted from  $700\text{ nm}$  ( $1.77\text{ eV}$ ) to  $760\text{ nm}$  ( $1.63\text{ eV}$ ) and  $846\text{ nm}$  ( $1.47\text{ eV}$ ).

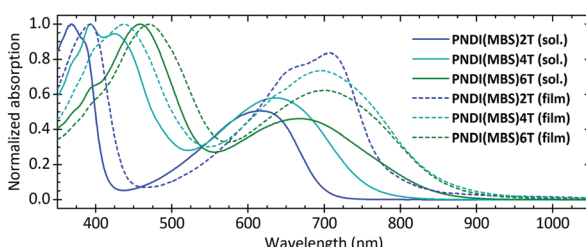


**Fig. 1** Normalized UV-vis absorption spectra of **PNDI(MBS)2T-6T** in CB ( $0.1\text{ g L}^{-1}$ ) and as annealed films.

In annealed thin films, a similar trend was observed for the onsets of the CT absorption bands, which shifted from  $783\text{ nm}$  ( $1.58\text{ eV}$ ) to  $855\text{ nm}$  ( $1.45\text{ eV}$ ) and  $864\text{ nm}$  ( $1.44\text{ eV}$ ). However, while the absorption maximum was following the same trend, the CT absorption peak did not; similar behaviour has been previously noted in donor–acceptor copolymers as the length of the donor was increased.<sup>21</sup>

In thin films, **PNDI(MBS)2T** showed the most redshifted peak at  $706\text{ nm}$ , redshifted by  $89\text{ nm}$  compared to solution and very close to the peak of **PNDI(2OD)2T** at  $705\text{ nm}$  (Fig. S9, ESI<sup>†</sup>). For **PNDI(MBS)4T** and **PNDI(MBS)6T**, the smaller redshifts of  $61$  and  $32\text{ nm}$  resulted in peaks at  $697$  and  $699\text{ nm}$ , respectively. Comparison of annealed and pristine films revealed little influence of the annealing on the spectra (Fig. S12, ESI<sup>†</sup>).

Photoluminescence spectra (Fig. 2) in CB showed a pronounced shift of the emission maximum from  $828\text{ nm}$  for **PNDI(2OD)2T** to  $716\text{ nm}$  for **PNDI(MBS)2T** and a significant increase in intensity. Measuring **PNDI(2OD)2T** in CN for reduced aggregation shifted its emission maximum to a similar wavelength of  $721\text{ nm}$  and increased the intensity, confirming that the differences in CB can be attributed to reduced aggregation as a result of the MBS. In contrast to **PNDI(MBS)2T**, **PNDI(MBS)4T** and **PNDI(MBS)6T** were found to be very weak emitters, possibly due to the increased oligothiophene length leading to enhanced relaxation of the excited state *via* inter-annular rotations.<sup>22</sup> Similar observations were made at lower concentration (Fig. S13, ESI<sup>†</sup>).

Cyclic voltammetry (CV) measurements of drop-cast films (Fig. 3) revealed that the half-wave potential in the reduction

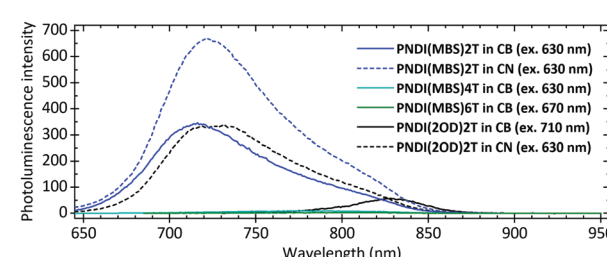


**Fig. 2** Photoluminescence spectra of **PNDI(MBS)2T-6T** and **PNDI(2OD)2T** in chlorobenzene (CB) and chloronaphthalene (CN). Conc.:  $0.1\text{ g L}^{-1}$ .



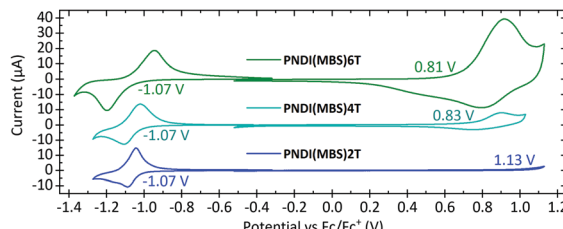


Fig. 3 Cyclic voltammetry measurements of drop-cast thin films of **PNDI(MBS)2T-6T** on ITO electrodes.

Table 1 UV-vis absorption and cyclic voltammetry data

| Polymer            | $\lambda_{\text{max,sol.}}^a$<br>(nm) | $\lambda_{\text{max,film}}^b$<br>(nm) | $E_{\text{g, opt}}^b$<br>(eV) | $E_{\text{Homo}}^{bc}$<br>(eV) | $E_{\text{Lumo}}^{bc}$<br>(eV) |
|--------------------|---------------------------------------|---------------------------------------|-------------------------------|--------------------------------|--------------------------------|
| <b>PNDI(MBS)2T</b> | 368/617                               | 393/706                               | 1.58                          | -5.93                          | -3.73                          |
| <b>PNDI(MBS)4T</b> | 394/636                               | 437/697                               | 1.45                          | -5.63                          | -3.73                          |
| <b>PNDI(MBS)6T</b> | 457/667                               | 470/699                               | 1.44                          | -5.61                          | -3.73                          |

<sup>a</sup> From measurements in chlorobenzene. <sup>b</sup> From film measurements.

<sup>c</sup> Estimated from CV measurements using ferrocene as the reference.

measurements of **PNDI(MBS)2T-6T** is unaffected by the increased density of thiophene units. The redox potential was determined to be -1.07 V vs. ferrocene/ferrocene<sup>+</sup> (Fc/Fc<sup>+</sup>) for all three polymers, which corresponds to an estimated lowest unoccupied molecular orbital (LUMO) energy level of -3.73 eV (Table 1) and indicates that the LUMO is dominated by the NDI units of the polymers. For estimating the highest occupied molecular orbital (HOMO) energy levels, we determined the redox potentials from the inflection points in the oxidation measurements. In contrast to the half-wave potentials in the reduction measurements, the redox potentials in the oxidation measurements shifted from 1.13 V to 0.83 V and 0.81 V vs. Fc/Fc<sup>+</sup>, corresponding to estimated HOMO energy levels of -5.93 eV, -5.63 eV and -5.61 eV, respectively. As for the optical bandgap, the redox potentials of **PNDI(MBS)4T** and **PNDI(MBS)6T** are very similar. However, while the peak currents in the reduction measurements are similar as well, the anodic peak current in the oxidation measurements increased drastically when increasing the density of thiophene units.

In conclusion, we can report that the attachment of the multibranched aliphatic side chain (MBS) 4-decyl-2-(2-decyldodecyl)hexadecyl to the backbone of conjugated polymers can have a drastic effect on the polymer properties. We attached the MBS to donor-acceptor copolymers composed of naphthalene diimide (NDI) and thiophene units and found it to drastically reduce the aggregation and blueshift the absorption and photoluminescence of **PNDI(MBS)2T** compared to the well-investigated polymer **PNDI(2OD)2T**, while retaining the excellent thermal stability. The MBS has an impressively high solubilizing capability, as we could demonstrate by increasing the number of unsubstituted thiophene units per side chain-substituted NDI unit in our set of polymers from two (in **PNDI(MBS)2T**) to four and six (in **PNDI(MBS)4T** and **PNDI(MBS)6T**). The high density of

unsubstituted, 'unshielded' thiophene units in the latter polymers has a pronounced effect on the oxidation in cyclic voltammetry (CV) measurements, significantly increasing the current and shifting the redox potential from 1.13 V to 0.81 V vs. Fc/Fc<sup>+</sup>. The redox potential of the reduction remained unaffected.

Considering the properties and facile synthesis of the MBS presented in this work, we believe it will find broad use in polymers for applications that benefit from reduced aggregation, increased solubility, and/or from a high density of unsubstituted, 'unshielded' aromatics in the polymer backbone.

We thank the EPSRC and Merck Chemicals for an iCase award and the Royal Society and the Wolfson Foundation (Royal Society Wolfson Fellowship) for funding. We further acknowledge funding from the European Union's Horizon 2020 research and innovation programme under the Marie Skłodowska-Curie grant agreement No. 796024.

## Conflicts of interest

There are no conflicts to declare.

## References

1. A. Facchetti, *Chem. Mater.*, 2011, **23**, 733–758.
2. A. C. Grimsdale, K. Leok Chan, R. E. Martin, P. G. Jokisz and A. B. Holmes, *Chem. Rev.*, 2009, **109**, 897–1091.
3. J. Mei and Z. Bao, *Chem. Mater.*, 2014, **26**, 604–615.
4. Z. Liu, G. Zhang and D. Zhang, *Acc. Chem. Res.*, 2018, **51**, 1422–1432.
5. Y. Yang, Z. Liu, G. Zhang, X. Zhang and D. Zhang, *Adv. Mater.*, 2019, **31**, 1903104.
6. H. Bronstein, C. B. Nielsen, B. C. Schroeder and I. McCulloch, *Nat. Rev. Chem.*, 2020, **4**, 66–77.
7. N. Blouin, A. Michaud and M. Leclerc, *Adv. Mater.*, 2007, **19**, 2295–2300.
8. H. Yan, Z. Chen, Y. Zheng, C. Newman, J. R. Quinn, F. Dötz, M. Kastler and A. Facchetti, *Nature*, 2009, **457**, 679–686.
9. C. Dai and B. Liu, *Energy Environ. Sci.*, 2020, **13**, 24–52.
10. X. Guo, F. S. Kim, M. J. Seger, S. A. Jenekhe and M. D. Watson, *Chem. Mater.*, 2012, **24**, 1434–1442.
11. J. Berlan, H. Delmas, I. Duée, J. L. Luche and L. Vuiglio, *Synth. Commun.*, 1994, **24**, 1253–1260.
12. S. Arseniyadis, K. S. Kyler and D. S. Watt, Addition and Substitution Reactions of Nitrile-Stabilized Carbanions, in *Organic Reactions*, ed. W. G. Dauben, John Wiley & Sons, Inc., 2005, vol. 31.
13. D. F. Taber and S. Kong, *J. Org. Chem.*, 1997, **62**, 8575–8576.
14. Z. Chen, Y. Zheng, H. Yan and A. Facchetti, *J. Am. Chem. Soc.*, 2009, **131**, 8–9.
15. A. Luzio, D. Fazzi, D. Natali, E. Giussani, K.-J. Baeg, Z. Chen, Y.-Y. Noh, A. Facchetti and M. Caironi, *Adv. Funct. Mater.*, 2014, **24**, 1151–1162.
16. M. M. Szumilo, E. H. Gann, C. R. McNeill, V. Lemaur, Y. Oliver, L. Thomsen, Y. Vaynzof, M. Sommer and H. Sirringhaus, *Chem. Mater.*, 2014, **26**, 6796–6804.
17. R. Matsidik, H. Komber, A. Luzio, M. Caironi and M. Sommer, *J. Am. Chem. Soc.*, 2015, **137**, 6705–6711.
18. L. Hu, J. Han, W. Qiao, X. Zhou, C. Wang, D. Ma, Y. Li and Z. Y. Wang, *Polym. Chem.*, 2018, **9**, 327–334.
19. R. Xie, A. R. Weisen, Y. Lee, M. A. Aplan, A. M. Fenton, A. E. Masucci, F. Kempe, M. Sommer, C. W. Pester, R. H. Colby and E. D. Gomez, *Nat. Commun.*, 2020, **11**, 893.
20. R. Steyrllethner, M. Schubert, I. Howard, B. Klaumünzer, K. Schilling, Z. Chen, P. Saalfrank, F. Laquai, A. Facchetti and D. Neher, *J. Am. Chem. Soc.*, 2012, **134**, 18303–18317.
21. P. M. Beaujuge, C. M. Amb and J. R. Reynolds, *Acc. Chem. Res.*, 2010, **43**, 1396–1407.
22. S. C. Rasmussen, S. J. Evenson and C. B. McCausland, *Chem. Commun.*, 2015, **51**, 4528–4543.

